Electronic Supplementary Material (ESI) for Journal of Materials Chemistry A.

Supporting Information

Rational Design of Single-Atom Catalysts for Electrochemical Ammonia Synthesis via a Descriptor-Based Approach

Jun Long,[abc] Xiaoyan Fu,[abc] and Jianping Xiao*[c]

[a] *Department of Chemistry, Zhejiang University, 866 Yuhangtang Road, Hangzhou 310058, P.R. China.*

[b] *School of Science, Westlake University, Hangzhou, 310024, P. R. China.*

[c] *State Key Laboratory of Catalysis, Dalian Institute of Chemical Physics, Chinese Academy of Sciences, Zhongshan Road 457, Dalian 116023, P. R. China.*

**Corresponding author: xiao@dicp.ac.cn*

Table S1 The elementary steps for different NRR pathways

	end-on	**side-on**
distal	**Pathway distal-e:** $N_2(g)+H^++e^-\rightarrow *NNH(e)$ $*NNH(e)+H^++e^-\rightarrow *NNH_2(e)$ $*NNH_2(e)+H^++e^-\rightarrow *N+NH_3(g)$ $*N+H^++e^-\rightarrow *NH$ $*NH+H^++e^-\rightarrow *NH_2$ $*NH_2+H^++e^-\rightarrow NH_3(g)$	**Pathway distal-s:** $N_2(g)+H^++e^-\rightarrow *NNH(s)$ $*NNH(s)+H^++e^-\rightarrow *NNH_2(s)$ $*NNH_2(s)+H^++e^-\rightarrow *N+NH_3(g)$ $*N+H^++e^-\rightarrow *NH$ $*NH+H^++e^-\rightarrow *NH_2$ $*NH_2+H^++e^-\rightarrow NH_3(g)$
alternating	**Pathway alternating-e:** $N_2(g)+H^++e^-\rightarrow *NNH(e)$ $*NNH(e)+H^++e^-\rightarrow *HNNH(e)$ $*HNNH(e)+H^++e^-\rightarrow *HNNH_2(e)$ $*HNNH_2(e)+H^++e^-\rightarrow *H_2NNH_2(e)$ $*H_2NNH_2(e)+H^++e^-\rightarrow *NH_2+NH_3(g)$ $*NH_2+H^++e^-\rightarrow NH_3(g)$	**Pathway alternating-s:** $N_2(g)+H^++e^-\rightarrow *NNH(s)$ $*NNH(s)+H^++e^-\rightarrow *HNNH(s)$ $*HNNH(s)+H^++e^-\rightarrow *HNNH_2(s)$ $*HNNH_2(s)+H^++e^-\rightarrow *H_2NNH_2(s)$ $*H_2NNH_2(s)+H^++e^-\rightarrow *NH_2+NH_3(g)$ $*NH_2+H^++e^-\rightarrow NH_3(g)$
mix$_1$	**Pathway mix$_1$-e:** $N_2(g)+H^++e^-\rightarrow *NNH(e)$ $*NNH(e)+H^++e^-\rightarrow *NNH_2(e)$ $*NNH_2(e)+H^++e^-\rightarrow *HNNH_2(e)$ $*HNNH_2(e)+H^++e^-\rightarrow *NH+NH_3(g)$ $*NH+H^++e^-\rightarrow *NH_2$ $*NH_2+H^++e^-\rightarrow NH_3(g)$	**Pathway mix$_1$-s:** $N_2(g)+H^++e^-\rightarrow *NNH(s)$ $*NNH(s)+H^++e^-\rightarrow *NNH_2(s)$ $*NNH_2(s)+H^++e^-\rightarrow *HNNH_2(s)$ $*HNNH_2(s)+H^++e^-\rightarrow *NH+NH_3(s)$ $*NH+H^++e^-\rightarrow *NH_2$ $*NH_2+H^++e^-\rightarrow NH_3(g)$
mix$_2$	**Pathway mix$_2$-e:** $N_2(g)+H^++e^-\rightarrow *NNH(e)$ $*NNH(e)+H^++e^-\rightarrow *NNH_2(e)$ $*NNH_2(e)+H^++e^-\rightarrow *HNNH_2(e)$ $*HNNH_2(e)+H^++e^-\rightarrow *H_2NNH_2(e)$ $*H_2NNH_2(e)+H^++e^-\rightarrow *NH_2+NH_3(g)$ $*NH_2+H^++e^-\rightarrow NH_3(g)$	**Pathway mix$_2$-s:** $N_2(g)+H^++e^-\rightarrow *NNH(s)$ $*NNH(s)+H^++e^-\rightarrow *NNH_2(s)$ $*NNH_2(s)+H^++e^-\rightarrow *HNNH_2(s)$ $*HNNH_2(s)+H^++e^-\rightarrow *H_2NNH_2(s)$ $*H_2NNH_2(s)+H^++e^-\rightarrow *NH_2+NH_3(g)$ $*NH_2+H^++e^-\rightarrow NH_3(g)$
mix$_3$	**Pathway mix$_3$-e:** $N_2(g)+H^++e^-\rightarrow *NNH(e)$ $*NNH(e)+H^++e^-\rightarrow *HNNH(e)$ $*HNNH(e)+H^++e^-\rightarrow *HNNH_2(e)$ $*HNNH_2(e)+H^++e^-\rightarrow *NH+NH_3(g)$ $*NH+H^++e^-\rightarrow *NH_2$ $*NH_2+H^++e^-\rightarrow NH_3(g)$	**Pathway mix$_3$-s:** $N_2(g)+H^++e^-\rightarrow *NNH(s)$ $*NNH(s)+H^++e^-\rightarrow *HNNH(s)$ $*HNNH(s)+H^++e^-\rightarrow *HNNH_2(s)$ $*HNNH_2(s)+H^++e^-\rightarrow *NH+NH_3(g)$ $*NH+H^++e^-\rightarrow *NH_2$ $*NH_2+H^++e^-\rightarrow NH_3(g)$

* represents the active site. "(e)" and "(s)" indicate the end-on and side-on adsorption respectively. For convenience, the successive mechanism for *NNH formation is not expressed in this table.

Table S2 Adsorption energies (E_{ads}) of $^*N_2$ and *H on the heteroatom-doped sites and metal sites for MB_4 and MN_4

	$E_{ads}(N_2)$ / eV		**$E_{ads}(^*H)$ / eV**	
	Doped site	Metal site[#]	Doped site	Metal site
WB_4	-0.55	-1.28	0.57	-0.5
MoB_4	-0.33	-0.92	0.58	-0.03
OsB_4	-0.01	-0.95	0.27	-0.09
FeB_4	-0.02	-1.11	0.35	0.16
RuB_4	-0.01	-0.81	0.31	0.39
RhB_4	-0.02	-0.42	0.34	0.48
WN_4	-0.01	-1.67	0.82	-1.04
MoN_4	-0.02	-1.59	0.66	-0.95
OsN_4	-0.01	-0.94	0.97	-0.75
FeN_4	-0.01	-0.99	1.08	-0.36
RuN_4	0.01	-0.24	1.06	-0.73
RhN_4	0.01	-0.01	1.26	-0.36

[#] The N_2 adsorption energies on metal sites is taken from the lower one between end-on and side-on adsorption.

Table S3 End-on adsorption energies of NRR intermediates on the studied SACs (eV)

	***N**	***NH**	***NH$_2$**	***N$_2$-e**	***NNH-e**	***NNH$_2$-e**	***HNNH-e**	***HNNH$_2$-e**	***H$_2$NNH$_2$-e**
CuC$_4$	5.58	3.43	1.06	-0.02	2.14	2.25	1.51	1.5	0.27
NiC$_4$	3.34	1.6	0.03	-0.01	1.01	1.06	0.99	0.61	0.03
PdC$_4$	3.13	1.47	0.00	-0.01	1.21	1.03	0.89	0.67	-0.13
RhC$_4$	0.93	0.52	-0.91	-0.21	0.69	0.36	0.45	-0.06	-0.35
RuC$_4$	0.51	-0.12	-1.08	-0.27	0.68	0.24	0.43	0.00	-0.54
FeC$_4$	0.39	0.02	-1.01	-0.52	0.29	0.14	0.34	-0.32	-0.58
OsC$_4$	-0.07	-0.8	-1.65	-0.48	0.27	-0.22	0.16	-0.65	-0.53
MoC$_4$	0.23	-0.96	-1.7	-0.52	0.05	-0.54	0.1	-0.74	-0.61
WC$_4$	-0.12	-1.61	-2.28	-0.68	-0.33	-1.01	-0.22	-1.22	-0.83
WB$_4$	-0.21	-1.95	-2.37	-1.15	-0.73	-1.44	-0.55	-1.72	-1.02
MoB$_4$	-0.31	-1.26	-1.72	-0.92	-0.28	-0.82	-0.17	-1.14	-0.79
OsB$_4$	0.28	-0.68	-1.52	-0.95	0.36	-0.5	-0.02	-0.5	-0.94
FeB$_4$	0.44	-0.67	-1.65	-1.11	-0.33	-0.77	-0.08	-0.71	-1.02
RuB$_4$	0.88	-0.07	-0.99	-0.81	0.31	-0.03	0.25	-0.06	-0.79
RhB$_4$	2.62	1.23	-0.84	-0.42	0.82	0.51	0.54	0.06	-0.69
WN$_4$	-1.99	-3.05	-2.83	-0.99	-1.38	-2.26	-0.71	-2.07	-1.1
MoN$_4$	-2.03	-2.83	-2.72	-1.2	-1.22	-2.11	-0.69	-1.98	-0.96
OsN$_4$	-0.88	-0.65	-1.16	-0.94	0.01	-0.47	-0.13	-0.42	-0.49
FeN$_4$	1.14	0.49	-0.75	-0.99	0.29	0.04	0.01	-0.02	-0.54
RuN$_4$	0.53	-0.28	-1.06	-0.01	0.06	-0.37	-0.21	-0.27	-0.63
RhN$_4$	3.32	1.81	-0.11	-0.01	0.97	1.57	1.27	0.51	0.2

Table S4 Side-on adsorption energies of NRR intermediates on SACs (eV)

	$^*N_2$-s[#]	***NNH-s**	**$^*NNH_2$-s**	***HNNH-s**	**$^*HNNH_2$-s**	**$^*H_2NNH_2$-s**
CuC_4	/	2.38	2.27	2.31	1.39	0.24
NiC_4	/	1.47	1.08	1.77	0.61	0.08
PdC_4	-0.01	1.54	1.48	1.12	0.62	-0.12
RhC_4	0.09	0.83	0.72	0.66	-0.35	-0.39
RuC_4	/	0.74	0.25	0.57	-0.39	-0.55
FeC_4	/	0.49	0.47	0.46	-0.51	-0.31
OsC_4	-0.48	0.33	-0.26	0.16	-0.77	-0.66
MoC_4	-0.28	0.15	-0.39	-0.22	-1.07	-0.59
WC_4	-0.57	-0.14	-1.07	-0.79	-1.54	-0.85
WB_4	-1.28	-0.78	-1.27	-1.15	-1.75	-0.98
MoB_4	-0.89	-0.17	-0.79	-0.46	-1.1	-0.78
OsB_4	-0.3	0.42	-0.1	-0.08	-0.63	-0.77
FeB_4	-0.55	0.13	-0.36	-0.09	-0.71	-0.6
RuB_4	-0.21	0.62	0.36	0.31	-0.57	-0.61
RhB_4	/	0.81	0.87	0.53	-0.09	-0.46
WN_4	-1.67	-1.93	-2	-1.72	-2.05	-1.1
MoN_4	-1.59	-1.58	-1.84	-1.48	-1.97	-0.96
OsN_4	-0.03	0.69	-0.48	0.78	-0.42	-0.49
FeN_4	-0.01	1.03	0.04	0.93	-0.02	-0.53
RuN_4	-0.24	0.85	-0.37	0.68	-0.27	-0.54
RhN_4	-0.01	1.07	1.58	1.46	0.51	0.19

[#] On some SASs, such as CuC_4, N_2 can't be adsorbed in side-on configuration, hence the corresponding adsorption energies are absent.

Table S5 End-on adsorption free energies of NRR intermediates on SACs (eV)

	***N**	***NH**	***NH$_2$**	***N$_2$-e**	***NNH-e**	***NNH$_2$-e**	***HNNH-e**	***HNNH$_2$-e**	***H$_2$NNH$_2$-e**
CuC$_4$	5.835	4.01	1.905	0.42	3.015	3.51	2.7	3.135	2.26
NiC$_4$	3.575	1.86	0.915	0.43	1.865	2.27	2.26	2.225	2.09
PdC$_4$	3.325	1.74	0.905	0.43	2.065	2.25	2.16	2.295	1.92
RhC$_4$	1.195	0.72	0.005	0.23	1.555	1.57	1.74	1.555	1.67
RuC$_4$	0.745	0.16	-0.205	0.17	1.555	1.45	1.62	1.625	1.44
FeC$_4$	0.645	0.26	-0.165	-0.08	1.175	1.41	1.64	1.315	1.41
OsC$_4$	0.185	-0.53	-0.765	-0.04	1.135	0.99	1.42	0.935	1.46
MoC$_4$	0.495	-0.68	-0.805	-0.08	0.955	0.73	1.33	0.905	1.25
WC$_4$	0.125	-1.34	-1.365	-0.24	0.565	0.22	1.02	0.425	1.17
WB$_4$	0.045	-1.69	-1.485	-0.71	0.145	-0.21	0.69	-0.075	0.97
MoB$_4$	-0.055	-1	-0.835	-0.48	0.595	0.41	1.07	0.505	1.2
OsB$_4$	0.535	-0.42	-0.635	-0.51	1.235	0.73	1.22	1.125	1.05
FeB$_4$	0.695	-0.41	-0.765	-0.67	0.545	0.46	1.16	0.915	0.97
RuB$_4$	1.135	0.19	-0.105	-0.37	1.185	1.2	1.5	1.565	1.2
RhB$_4$	2.875	1.49	0.045	0.02	1.695	1.74	1.79	1.685	1.3
WN$_4$	-1.735	-2.79	-1.945	-0.55	-0.505	-1.03	0.54	-0.445	0.89
MoN$_4$	-1.775	-2.57	-1.835	-0.76	-0.345	-0.88	0.56	-0.355	1.03
OsN$_4$	-0.625	-0.39	-0.275	-0.5	0.915	0.76	1.12	1.205	1.5
FeN$_4$	1.395	0.75	0.135	-0.55	1.165	1.27	1.26	1.605	1.45
RuN$_4$	0.785	-0.02	-0.175	0.43	0.935	0.86	1.04	1.355	1.36
RhN$_4$	3.575	2.07	0.775	0.43	1.845	2.8	2.52	2.135	2.19

Table S6 Side-on adsorption free energies of NRR intermediates (eV)

	$*N_2$-s[#]	***NNH-s**	**$*NNH_2$-s**	***HNNH-s**	**$*HNNH_2$-s**	**$*H_2NNH_2$-s**
CuC_4	/	3.255	3.53	3.5	3.025	2.23
NiC_4	/	2.325	2.29	3.04	2.225	2.14
PdC_4	0.43	2.395	2.7	2.39	2.245	1.93
RhC_4	0.53	1.695	1.93	1.95	1.265	1.63
RuC_4	/	1.615	1.46	1.76	1.235	1.43
FeC_4	/	1.375	1.74	1.76	1.125	1.68
OsC_4	-0.04	1.195	0.95	1.42	0.815	1.33
MoC_4	0.16	1.055	0.88	1.01	0.575	1.27
WC_4	-0.13	0.755	0.16	0.45	0.105	1.15
WB_4	-0.84	0.095	-0.04	0.09	-0.105	1.01
MoB_4	-0.45	0.705	0.44	0.78	0.545	1.21
OsB_4	0.14	1.295	1.13	1.16	0.995	1.22
FeB_4	-0.11	1.005	0.87	1.15	0.915	1.39
RuB_4	0.23	1.495	1.59	1.56	1.055	1.38
RhB_4	/	1.685	2.1	1.78	1.535	1.53
WN_4	-1.23	-1.055	-0.77	-0.47	-0.425	0.89
MoN_4	-1.15	-0.705	-0.61	-0.23	-0.345	1.03
OsN_4	0.41	1.595	0.75	2.03	1.205	1.5
FeN_4	0.43	1.905	1.27	2.18	1.605	1.46
RuN_4	0.2	1.725	0.86	1.93	1.355	1.45
RhN_4	0.43	1.945	2.81	2.71	2.135	2.18

[#] On some SASs, such as NiC_4, N_2 can’t be adsorbed in side-on configuration, hence the corresponding adsorption free energies are absent.

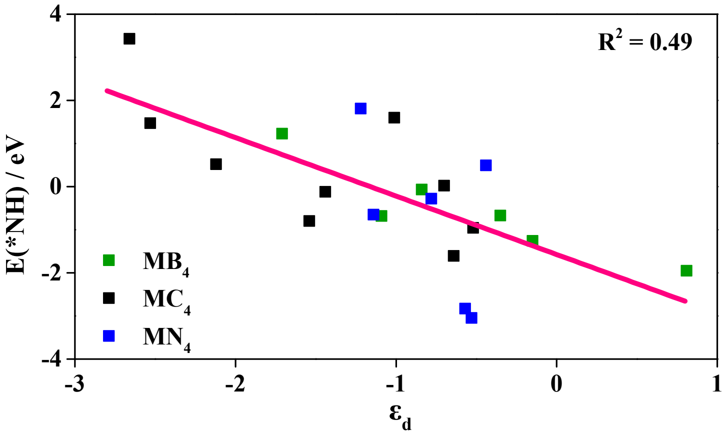

Fig. S1 Correlation between E(*NH) and d band center (ε_d)

Note1: Calculation of φ

In previous study[1], the parameter φ was defined as $\varphi = \theta_d \times \frac{E_M + \alpha(n_C \times E_C + n_N \times E_N)}{E_O(or\ E_H)}$ to describe the adsorption energy of *OH and *H, respectively. The numerator "$E_M + \alpha(n_C \times E_C + n_C \times E_N)$" can represent the total electronegativity of metal atom and its coordination environment. E_O and E_H are electronegativity of the attachment atoms in adsorbed *OH and *H. θ_d is the valence electrons of d orbital of metal atom. Hence, the term $\frac{E_M + \alpha(n_C \times E_C + n_N \times E_N)}{E_O(or\ E_H)}$ can indicate the ratio of θ_d possessed by the active center of SACs after the electron interaction between metal atom and adsorbates.

In this study, the reaction intermediates of NRR are adsorbed to SACs with N atom, as shown in Fig. 1b, thus φ was calculated as the following formula in this study.

$$\varphi = \theta_d \times \frac{E_M + \alpha(n_C \times E_C + n_N \times E_N + n_B \times E_B)}{E_N} \tag{S1}$$

where θ_d represents the valence electrons in the occupied d orbital of the metal element; E_M, E_C, E_N and E_B are the electronegativity of metal, C, N and B elements; n_C, n_N and n_B represent the number of nearest-neighbour C, N and B atoms; α is correction coefficient and set to 1 here. The θ_d, E_M, E_C, E_N, E_B and calculated value of φ were listed in Table S7.

Table S7 The values of θ_d, E_M, E_C, E_N, E_B and φ

SACs	θ_d	E_M	E_N	E_C	E_B	φ
WC_4	4	2.36	3.04	2.55	2.04	16.52632
MoC_4	5	2.16	3.04	2.55	2.04	20.32895
OsC_4	6	2.18	3.04	2.55	2.04	24.43421
FeC_4	6	1.83	3.04	2.55	2.04	23.74342
RuC_4	7	2.2	3.04	2.55	2.04	28.55263
RhC_4	8	2.28	3.04	2.55	2.04	32.84211
CuC_4	10	1.9	3.04	2.55	2.04	39.80263
NiC_4	8	1.92	3.04	2.55	2.04	31.89474
PdC_4	10	2.2	3.04	2.55	2.04	40.78947
WB_4	4	2.36	3.04	2.55	2.04	13.84211
MoB_4	5	2.16	3.04	2.55	2.04	16.97368
OsB_4	6	2.18	3.04	2.55	2.04	20.40789
FeB_4	6	1.83	3.04	2.55	2.04	19.71711
RuB_4	7	2.2	3.04	2.55	2.04	23.85526
RhB_4	8	2.28	3.04	2.55	2.04	27.47368
WN_4	4	2.36	3.04	2.55	2.04	19.10526
MoN_4	5	2.16	3.04	2.55	2.04	23.55263
OsN_4	6	2.18	3.04	2.55	2.04	28.30263
FeN_4	6	1.83	3.04	2.55	2.04	27.61184
RuN_4	7	2.2	3.04	2.55	2.04	33.06579
RhN_4	8	2.28	3.04	2.55	2.04	38

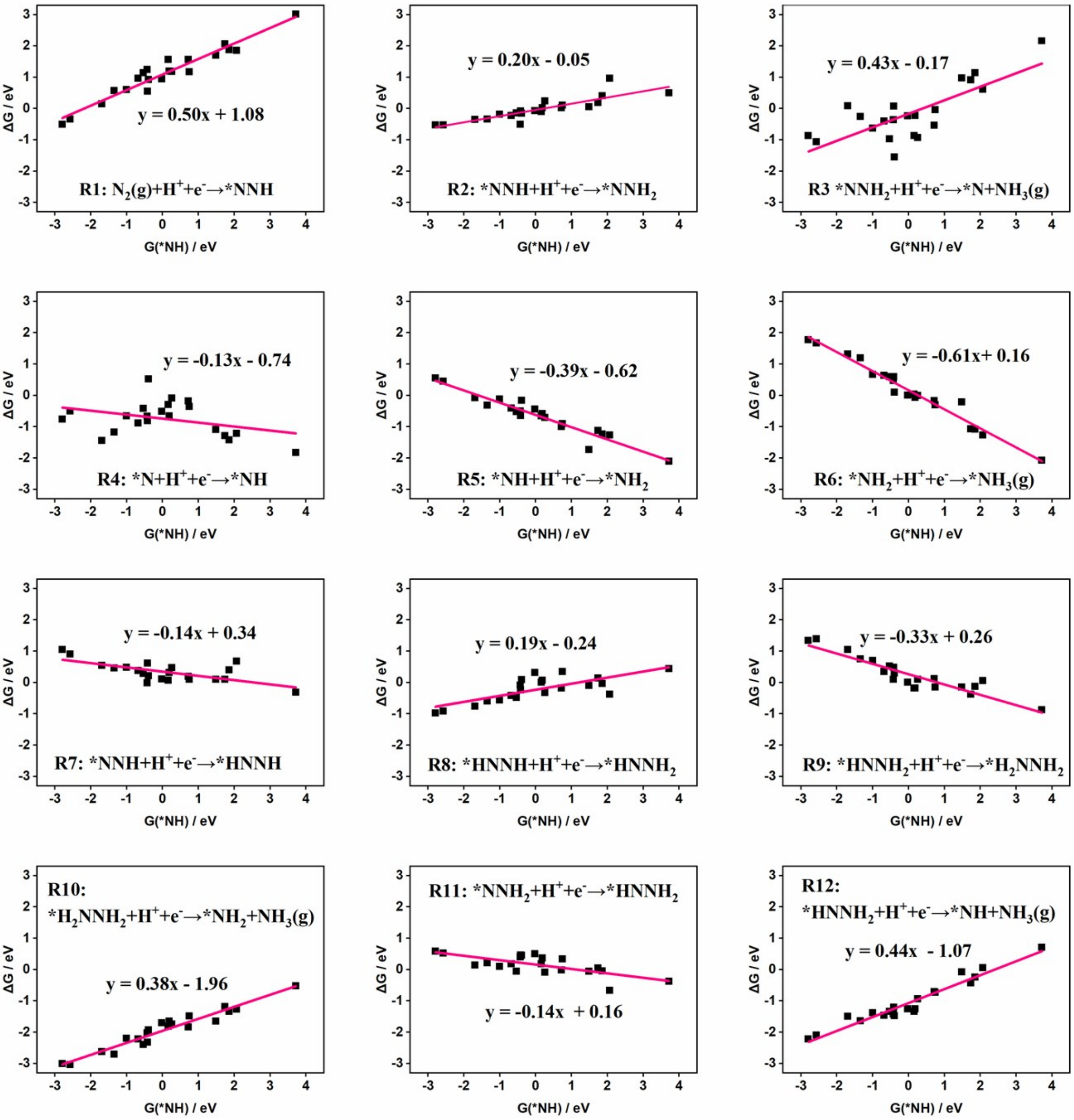

Fig. S2 Linear correlations between the reaction free energies of elementary steps and G(*NH) for end-on mechanism.

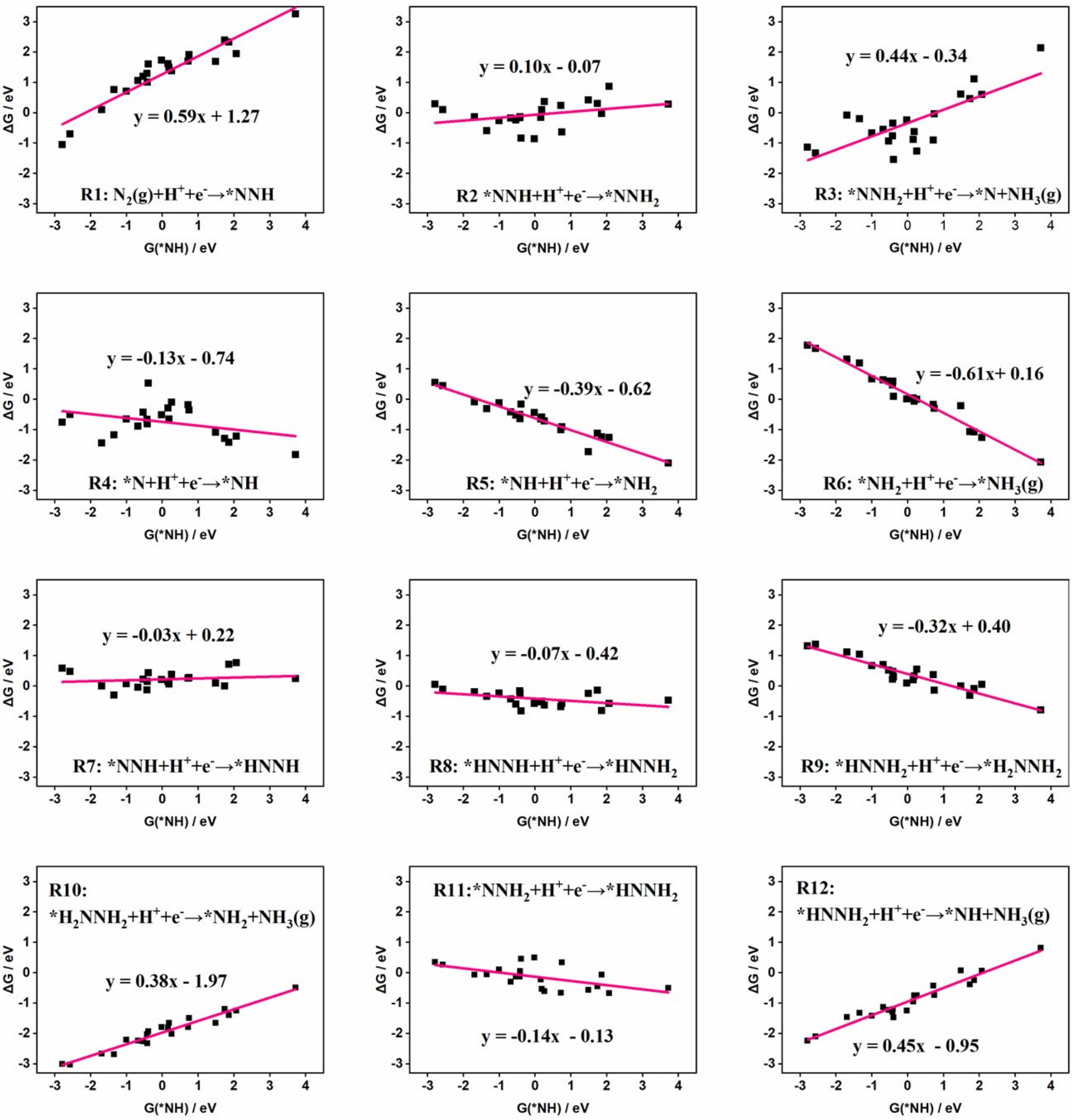

Fig. S3 Linear correlations between the reaction free energies of elementary steps and G(*NH) for side-on mechanism

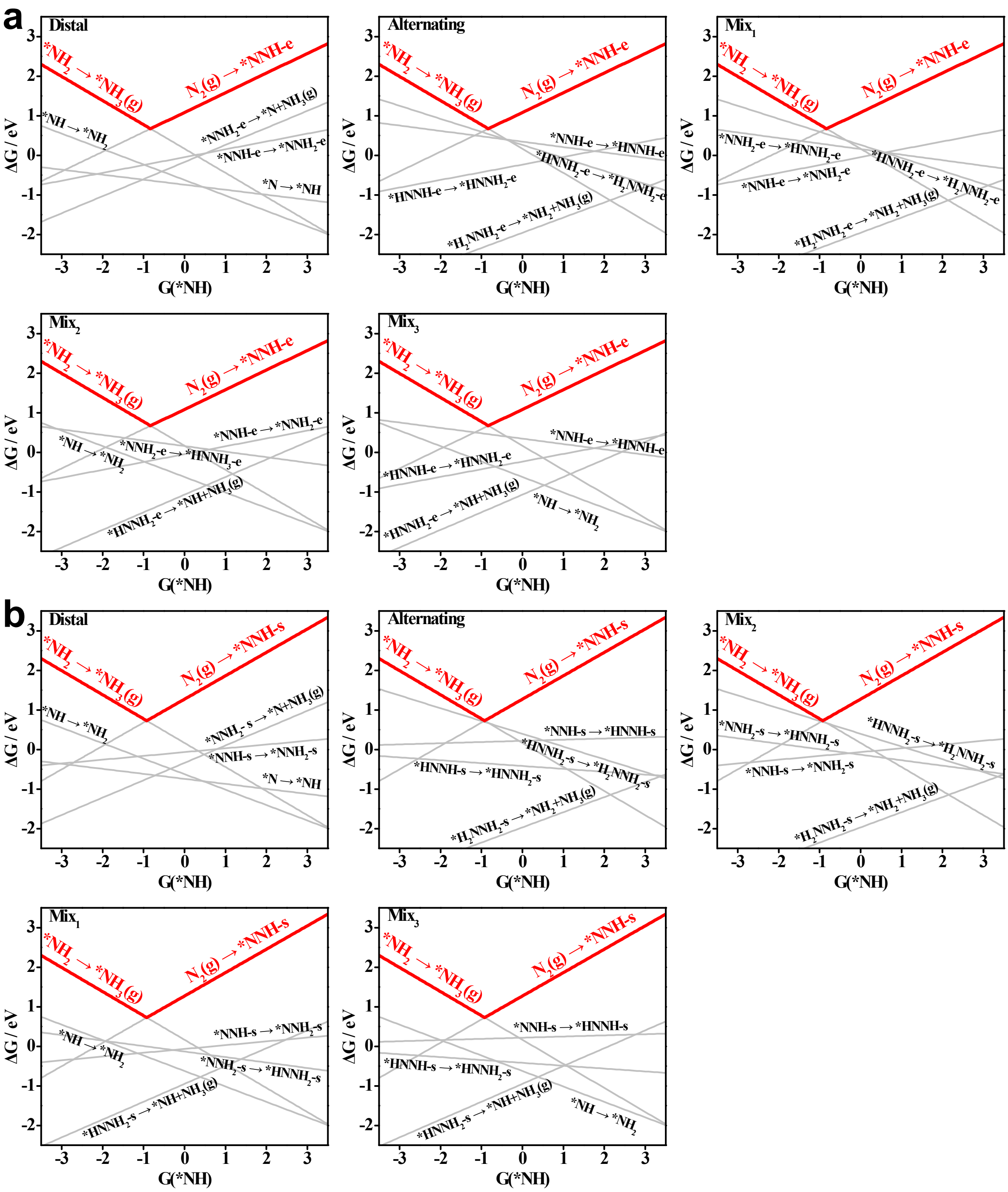

Fig. S4 Reaction free energies (ΔG) of elementary steps described linearly by the adsorption free energy of NH* for each pathway, where the red lines represent potential-determining steps. (a) end-on mechanism, (b) side-on mechanism. * represents the active site. "-e" and "-s" indicate the end-on and side-on adsorption, respectively. It can be found that the PDS of the five pathways are totally the same for end-on and side-on mechanisms, respectively.

Table S8 Elementary reactions in Fig. 3a and b

Reaction number	Elementary reactions
R1	$N_2(g) + H^+ + e^- \rightarrow {*NNH}$
R2	$*NNH + H^+ + e^- \rightarrow {*NNH_2}$
R3	$*NNH2 + H^+ + e^- \rightarrow {*N} + NH_3(g)$
R4	$*N + H^+ + e^- \rightarrow {*NH}$
R5	$*NH + H^+ + e^- \rightarrow {*NH_2}$
R6	$*NH_2 + H^+ + e^- \rightarrow {*NH_3(g)}$
R7	$*NNH + H^+ + e^- \rightarrow {*HNNH}$
R8	$*HNNH + H^+ + e^- \rightarrow {*HNNH_2}$
R9	$*HNNH_2 + H^+ + e^- \rightarrow {*H_2NNH_2}$
R10	$*H_2NNH_2 + H^+ + e^- \rightarrow {*NH_2} + NH_3(g)$
R11	$*NNH_2 + H^+ + e^- \rightarrow {*HNNH_2}$
R12	$*HNNH_2 + H^+ + e^- \rightarrow {*NH} + NH_3(g)$

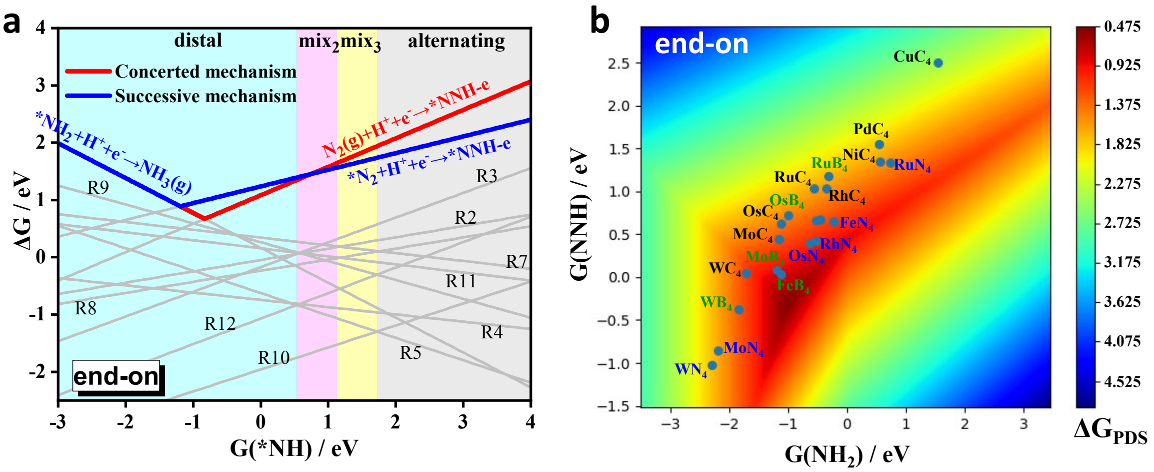

Fig. S5 (a) Reaction free energies of elementary steps as the function of G(*NH) for end-on mechanism. Red lines are the PDS of NRR when considering concerted *NNH formation mechanism and blue lines are that for successive mechanism. (b) Two-dimensional activity map of NRR for end-on mechanism when considering concerted *NNH formation.

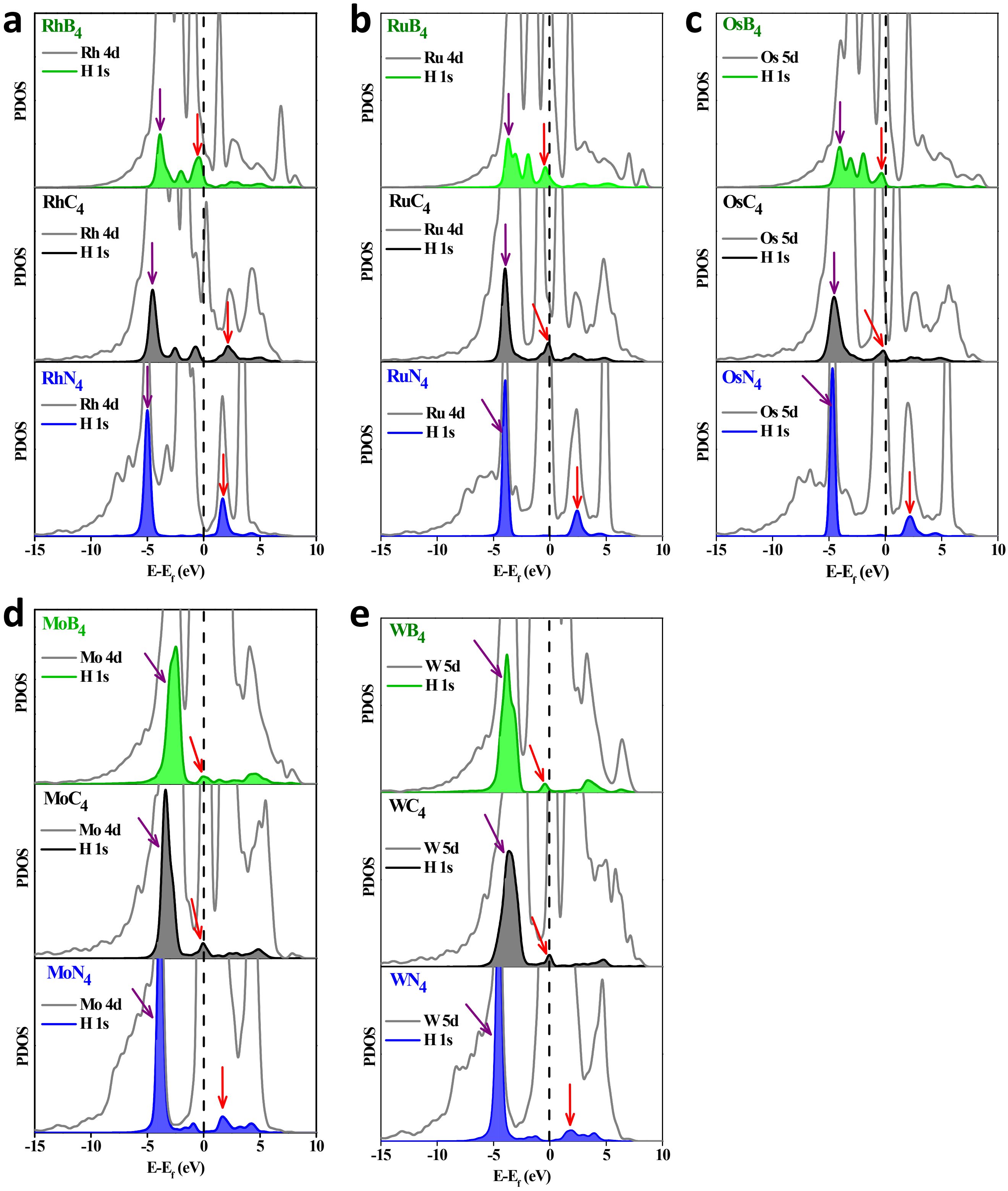

Fig. S6 Projected density of states (PDOS) analysis for H adsorbed on MB_4, MC_4 and MN_4.

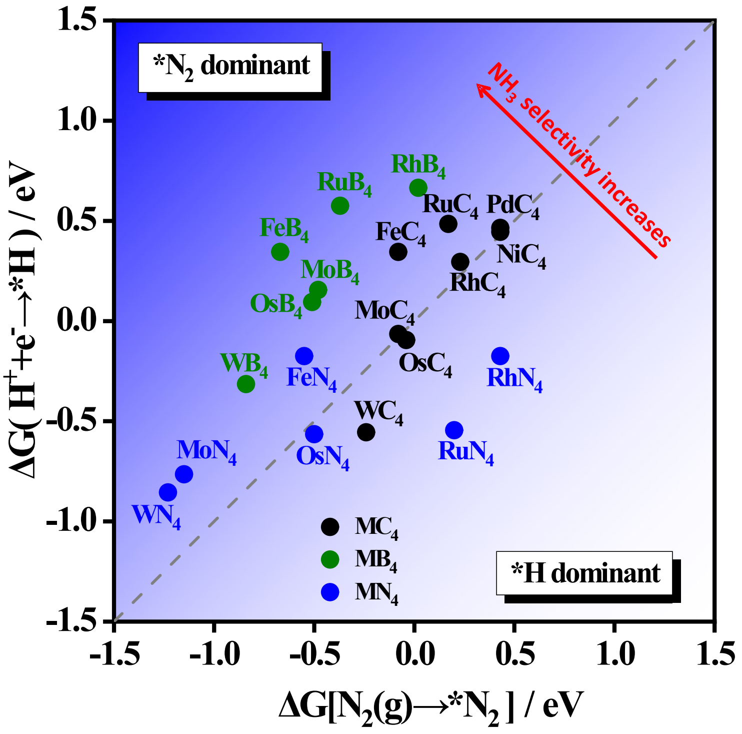

Fig. S7 $\Delta G[N_2(g)\rightarrow{}^*N_2]$ compared with $\Delta G(H^+ + e^- \rightarrow {}^*H)$

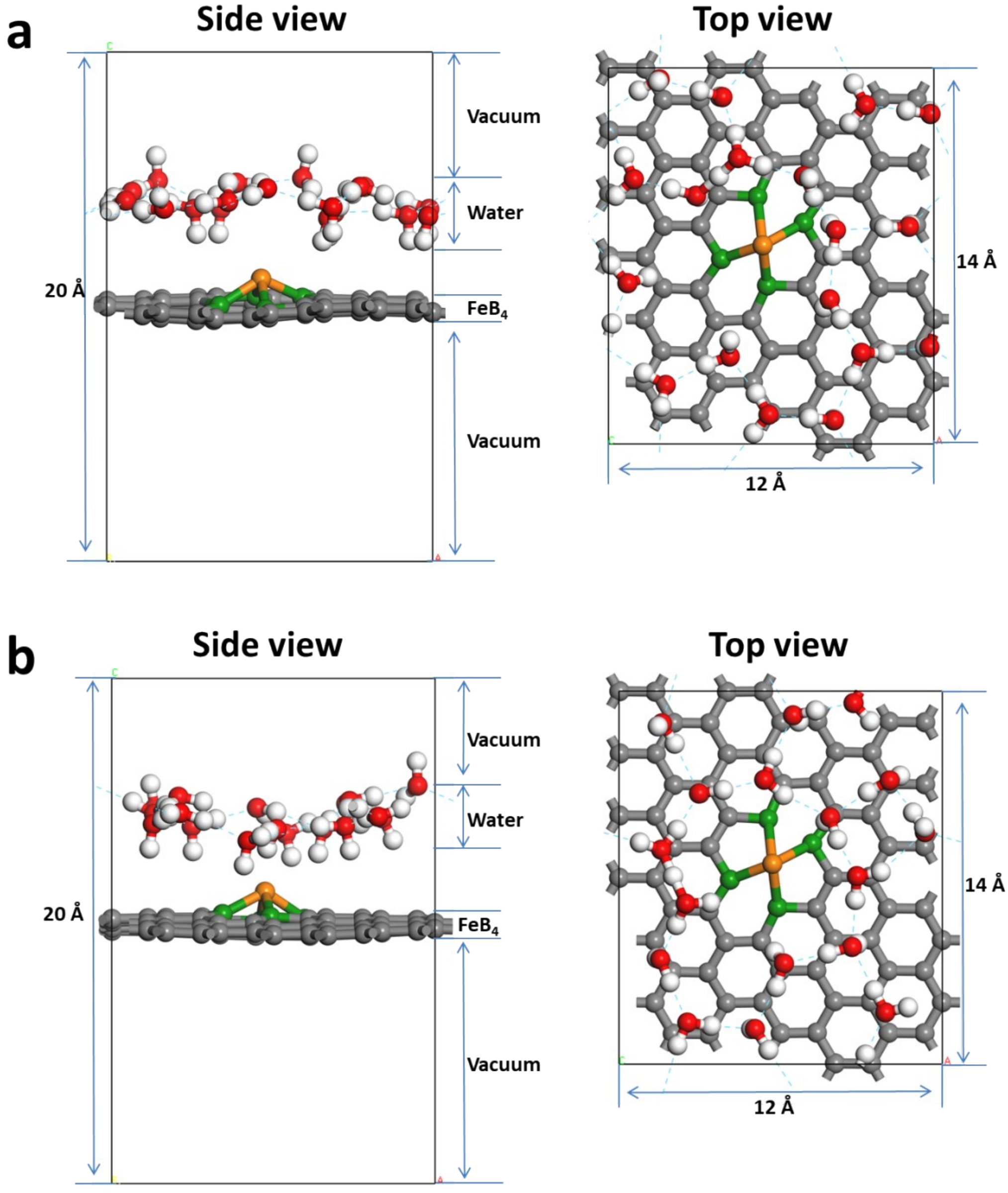

Fig. S8 (a) Water structure considered in this study to calculate all the activation energies of proton transfer reactions on FeB_4. MoB_4 has a similar water structure with FeB_4 and is not shown. (b) The comparative water structure to calculate the activation energy of N_2 protonation. The gray, green, blue, red, white and orange atoms are C, B, N, O, H and Fe. The dash line represent H-bond network.

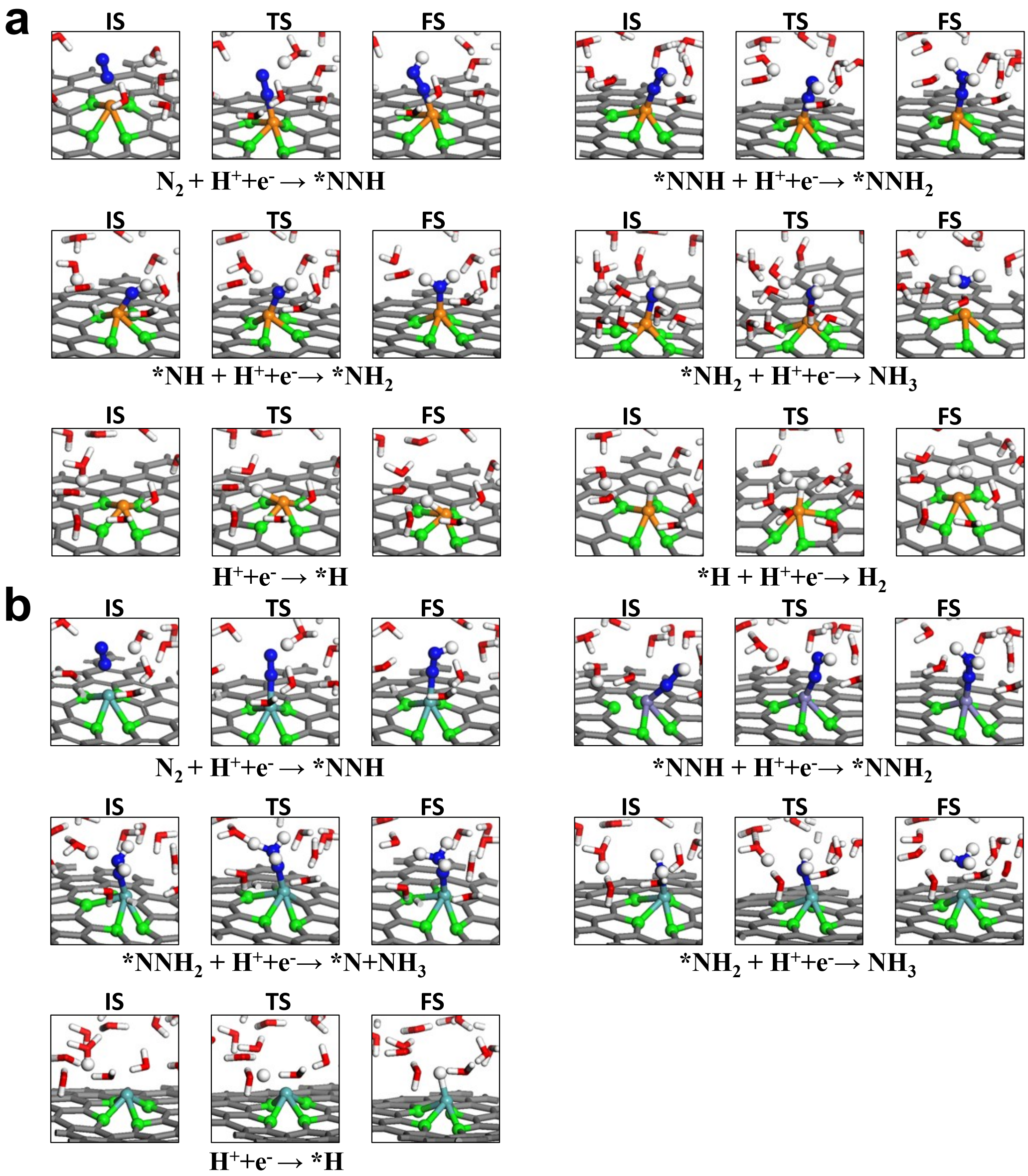

Fig. S9 Geometry structures of IS, TS and FS for elementary reactions of NRR and HER on FeB_4 (a) and MoB_4 (b). The gray, green, blue, red, white, orange and light blue atoms are C, B, N, O, H, Fe and Mo. For *NNH_2+H^++e^-→*N+NH_3 and *N+H^++e^-→*NH on FeB_4, *N+H^++e^-→*NH, *NH+H^++e^-→*NH_2, and *H+H^++e^-→H_2 on MoB_4, there are no TS found according to the results of CI-NEB. Hence they are not included in this Figure.

Note2: Potential-dependent energy barriers

The potential-dependent barriers in electrochemical process were estimated using a so-called “charge-extrapolation” method, proposed by Nørskov et al.[2-3] For an electrochemical reduction step, the transition state (TS) was found by the climbing image nudged elastic band (CI-NEB) method at first.[4-5] In this process, the total charge of system keeps constant while potential will change. For the electrochemical elementary reactions studied in this work, the calculated surface charge transfer (q) and potential (U) at initial state (IS), TS, and final state (FS) are plotted in Figure S6, which show good linear correlations. Based on those correlations, a capacitor model can be considered to calculate the barrier at constant potential[6].

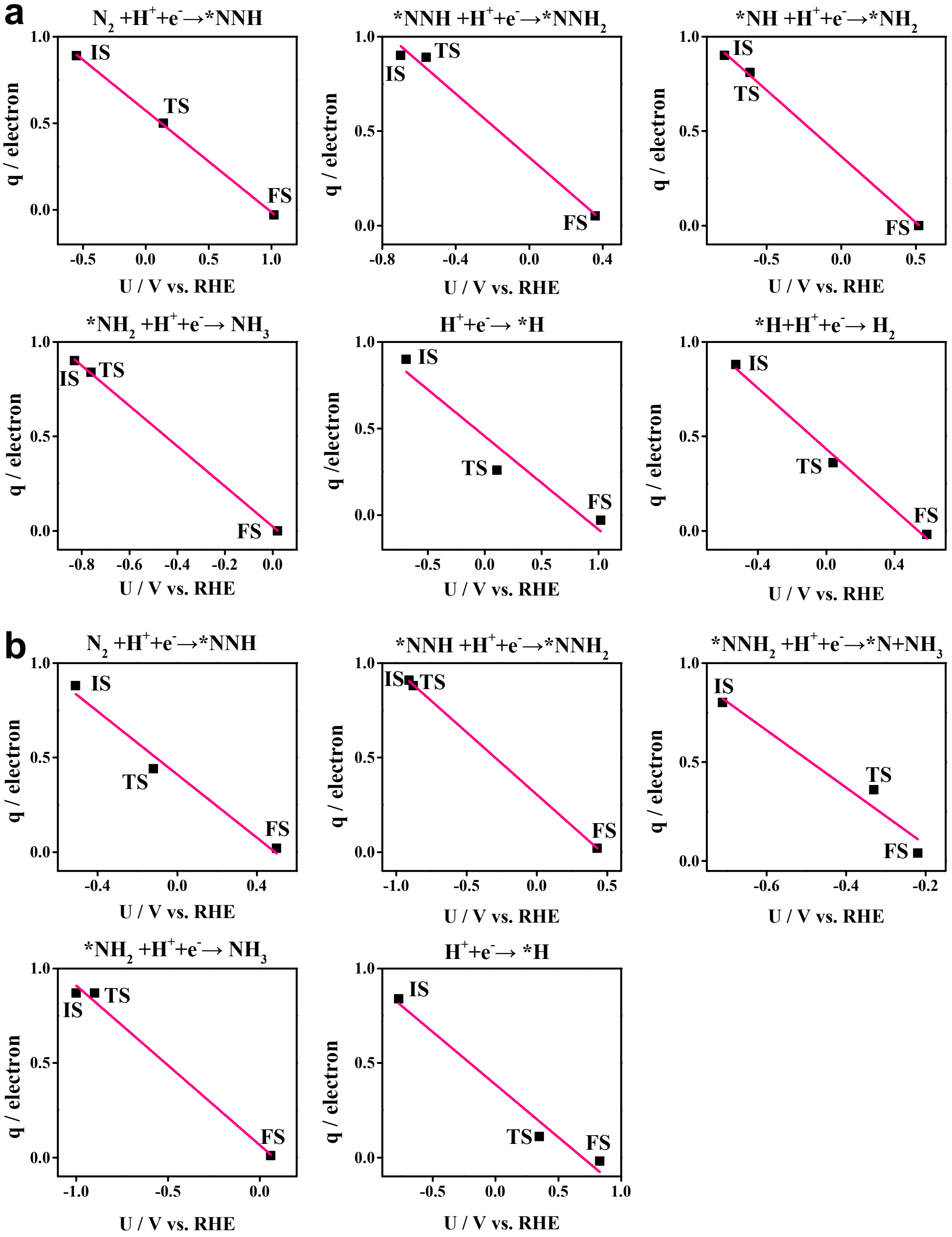

Figure S10. Calculated surface charge transfer (q) and potential (U) at IS, TS and FS for the elementary steps of NRR and HER for FeB_4 (a) and MoB_4 (b). There is no TS for $*NNH_2 + H^+ + e^- \rightarrow *N + NH_3$ and $*N + H^+ + e^- \rightarrow *NH$ on FeB_4, and for $*N + H^+ + e^- \rightarrow *NH$, $*NH + H^+ + e^- \rightarrow *NH_2$, and $*H + H^+ + e^- \rightarrow H_2$ on MoB_4, according to the results of CI-NEB. Hence they are not included in this Figure.

The IS and TS correspond to work functions Φ_1 and Φ_2, energies $E_1(\Phi_1)$ and $E_2(\Phi_2)$, and interfacial charges q_1 and q_2, respectively. The corresponding energy change between IS and TS at constant work functions, Φ_1 and Φ_2, are given by

$$E_2(\Phi_1) - E_1(\Phi_1) = E_2(\Phi_2) - E_1(\Phi_1) + \frac{(q_2 - q_1)(\Phi_2 - \Phi_1)}{2} \tag{S2}$$

$$E_2(\Phi_2) - E_1(\Phi_2) = E_2(\Phi_2) - E_1(\Phi_1) - \frac{(q_2 - q_1)(\Phi_2 - \Phi_1)}{2} \tag{S3}$$

Taking eq S2 − eq S1 and setting $\Delta E(\Phi) = E_2(\Phi) - E_1(\Phi)$ at a given work function Φ and $\Delta q = q2 - q1$, we obtain

$$\Delta E(\Phi_2) - \Delta E(\Phi_1) = -\Delta q(\Phi_2 - \Phi_1) \tag{S4}$$

where $\Delta E(\Phi_1)$ and $\Delta E(\Phi_2)$ represent the barriers at constant Φ_1 and Φ_2. Setting Φ_1 as the reference work function, Φ_{ref} (e.g., that corresponding to the standard hydrogen electrode potential), and Φ_2 to be the independent variable, we obtain the energy barriers as a function of Φ_2

$$\Delta E(\Phi_2) = \Delta E(\Phi_{ref}) - \Delta q(\Phi_2 - \Phi_{ref}) \tag{S5}$$

A specific Φ corresponds to a potential via $U_{SHE} = \frac{\Phi - \Phi_{SHE}}{e}$ and Φ_{SHE} has been determined experimentally to be ~4.44 eV[7]. In this way, the potential-dependent barrier can be calculated.

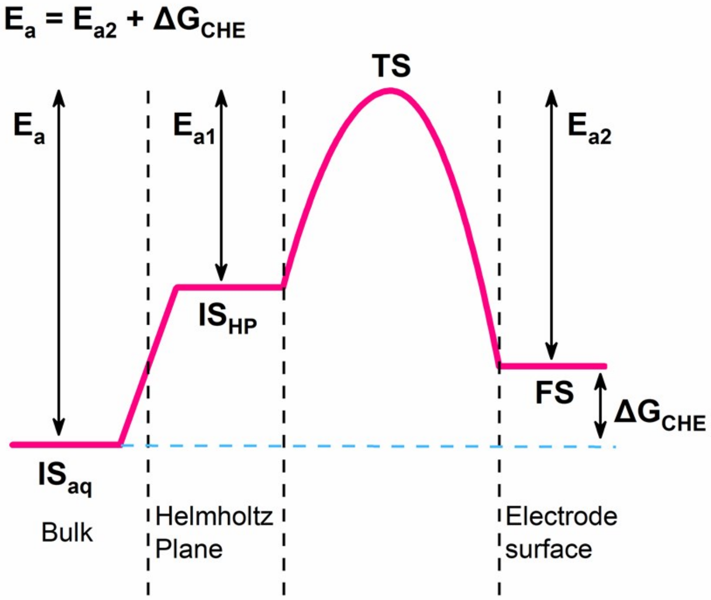

Fig. S11 Illustration for referencing the activation energy to bulk proton. E_{a2} referenced to FS is calculated via the charge-extrapolation method. ΔG_{CHE} is the reaction free energy acquired via computational hydrogen electrode (CHE). This scheme is reproduced from ref. 48.

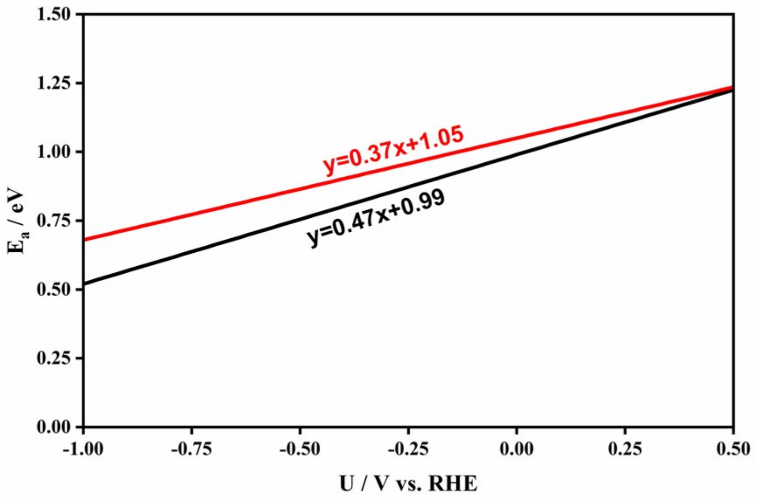

Fig. S12 Calculated activation energies of N_2 protonation on FeB_4 with the water structure used in this study (black line) and the comparative water structure (red line) at varying potentials.

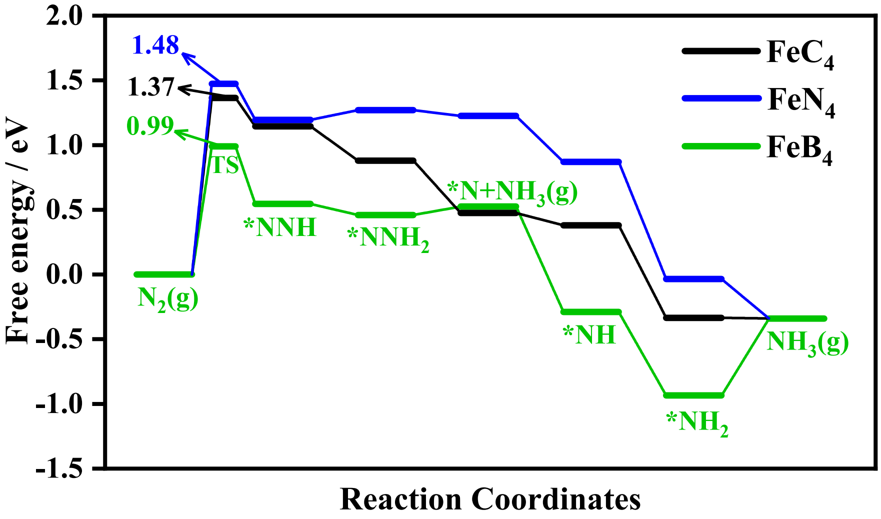

Fig. S13 Free energy diagrams of NRR on FeC_4, FeN_4 and FeB_4 at 0V vs. RHE

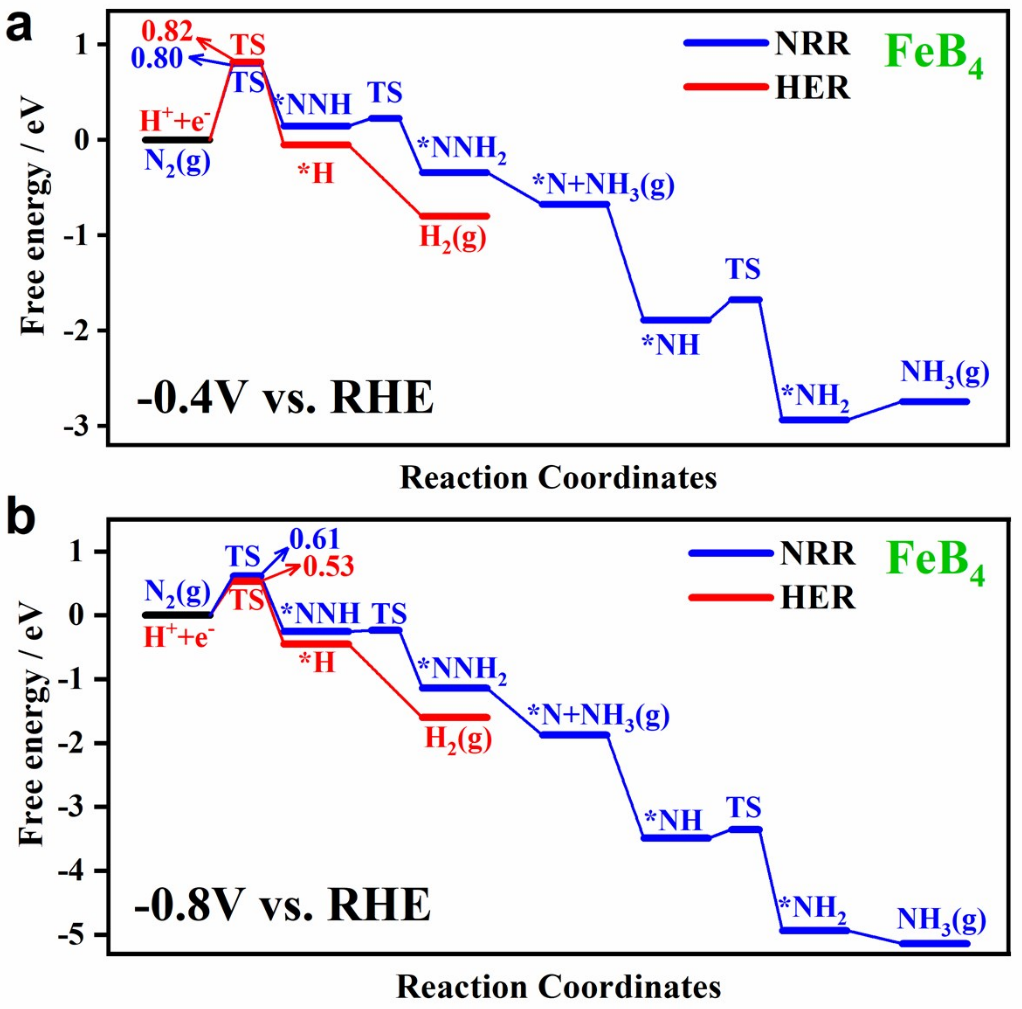

Fig. S14 Free energy diagram of NRR and HER on FeB4 at -0.4 (a) and -0.8 V vs. RHE

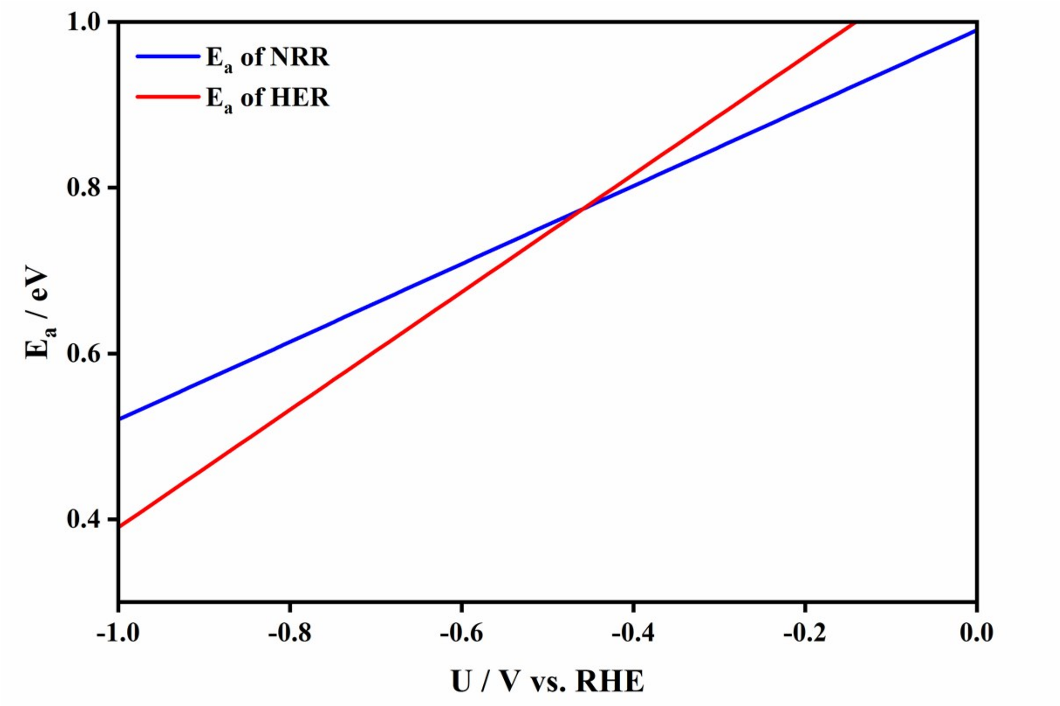

Fig. S15 Activation energies of NRR (blue line) and HER (red line) change with applied potential on FeB_4

Note3: Binding energy and cohesive energy

For FeB_4, the binding energy (E_b) of a single Fe atom on the graphene-based substrate (Fig. S16) was calculated as:

$$E_b = E_{SACs} - E_{substrate} - E_{Fe} \tag{S6}$$

where E_{SACs}, $E_{substrate}$ and E_{Fe} represent the total energy of FB_4 SACs, graphene-based substrate and a single Fe atom in vacuum, respectively.

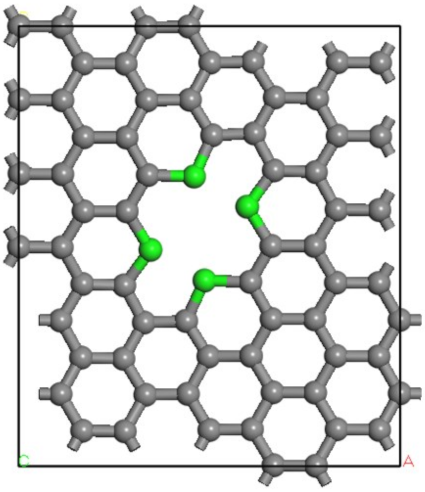

Fig. S16 Graphene-based substrate for FeB_4, where two C atoms of graphene are removed and the resulted 4 pyridine-type C atoms are substituted by B.

The cohesive energy (E_{coh}) of Fe bulk was calculated as :

$$E_{coh} = \frac{E_{bulk}}{n} - E_{Fe} \tag{S7}$$

where E_{bulk} and n indicate the total energy of unit cell of Fe and the number of Fe atom in the cell, respectively. E_{Fe} represents the total energy of a single Fe atom in vacuum.

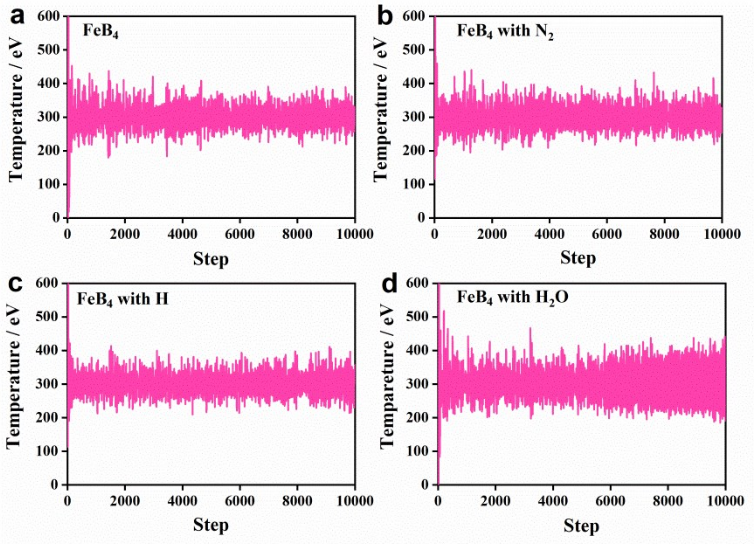

Fig. S17 Variations of temperatures for AIMD simulation of FeB_4 (a), FeB_4 with N_2 (b), H (c) and H_2O (d)

References

(1) Xu, H.; Cheng, D.; Cao, D.; Zeng, X. C., A universal principle for a rational design of single-atom electrocatalysts. *Nat. Catal.* **2018***, 1*, 339-348.

(2) Chan, K.; Norskov, J. K., Electrochemical Barriers Made Simple. *J. Phys. Chem. Lett.* **2015***, 6*, 2663-8.

(3) Chan, K.; Norskov, J. K., Potential Dependence of Electrochemical Barriers from ab Initio Calculations. *J. Phys. Chem. Lett.* **2016***, 7*, 1686-90.

(4) Henkelman, G., Improved tangent estimate in the nudged elastic band method for finding minimum energy paths and saddle points. *J. Chem. Phys.* **2000***, 113*, 9978-9985.

(5) Henkelman, G.; Uberuaga, B. P.; Jónsson, H., A climbing image nudged elastic band method for finding saddle points and minimum energy paths. *J. Chem. Phys.* **2000***, 113*, 9901-9904.

(6) Li, H.; Guo, C.; Fu, Q.; Xiao, J., Toward Fundamentals of Confined Electrocatalysis in Nanoscale Reactors. *J. Phys. Chem. Lett.* **2019***, 10*, 533-539.

(7) Trasatti, S., The Absolute Electrode Potential - An Explanatory Note (Recommendations 1986). *Pure Appl. Chem.* **1986,** *58*, 955-966.